Available online at www.sciencedirect.com

ScienceDirect

Nuclear Physics A 982 (2019) 607–610

www.elsevier.com/locate/nuclphysa

XXVIIth International Conference on Ultrarelativistic Nucleus-Nucleus Collisions (Quark Matter 2018)

Systematic Studies of Jet-medium Interactions in STAR

Kun Jiang (for the STAR Collaboration)[a,b]

[a] *Department of Modern Physics, University of Science and Technology of China, Hefei 230026, China*
[b] *Department of Physics and Astronomy, Purdue University, West Lafayette, Indiana 47907, USA*

Abstract

In these proceedings, we report recent jet results from STAR in heavy-ion collisions. The first measurement of centrality dependence of di-jet momentum imbalance A_J at RHIC is presented. An apparent evolution of the A_J distributions from central to peripheral collisions is observed. A new di-hadron correlation measurement with a method to subtract all orders of flow background using data themselves is also presented to study how the lost energy of jets is redistributed to particles with low-to-modest transverse momentum.

Keywords: di-jet imbalance, di-hadron correlations

1. Introduction

Energetic partons originating from initial hard scatterings lose energy due to interactions in the hot dense medium created in relativistic heavy-ion collisions. Experimentally, different trigger objects can be measured to select hard scattering events to study the partonic energy loss mechanisms [1]. These triggers include high-p_T particles, jets, direct-photon and so on. High-p_T particle triggers at RHIC might bias towards hard scatterings produced in the surface of the collision zone. The away-side partner jet therefore has an enhanced likelihood to traverse a large path length in the medium. Di-jet trigger has different bias. The di-jet selection if required hard hadrons on the recoil jet will have a preference to almost tangential di-jets which traverse the medium with a shorter but finite in-medium path length. The direct-photon trigger does not suffer the surface bias, since the photon mean free path is much larger than the size of the medium.

2. Di-jet Momentum Imbalance

Jets are reconstructed from charged tracks measured in the Time Projection Chamber (TPC) [2] and neutral particle information recorded by the Barrel Electromagnetic Calorimeter (BEMC) [3], using the anti-k_T algorithm from the FastJet package [4, 5]. To avoid double-counting the energy deposition in the BEMC from charged tracks, the transverse momentum of any charged track that extrapolates to a BEMC tower is subtracted from the transverse energy (E_T) of that tower. A tower energy is set to zero if the extrapolated track has a larger momentum than the tower energy. Events were selected by an online high tower (HT) trigger, which required $E_T > 5.4$ GeV in at least one BEMC tower. Event centrality is determined by the raw charged particle multiplicity in the TPC within the pseudorapidity range of $|\eta| < 0.5$, corrected for

https://doi.org/10.1016/j.nuclphysa.2018.12.011
0375-9474/© 2018 Published by Elsevier B.V.
This is an open access article under the CC BY-NC-ND license (http://creativecommons.org/licenses/by-nc-nd/4.0/).

luminosity and vertex position dependence. In the jet reconstruction, firstly, only tracks with $p_T > 2$ GeV/c are considered to minimize the background and combinatorial jets. We refer to this selection as (di-)jets with "hard cores". It is unnecessary to subtract the background energy since the median background energy density $\langle\rho\rangle$ is 0 at RHIC when only particles with $p_T > 2$ GeV/c are considered.

The di-jet momenta imbalance is defined as

$$A_J = (p_T^{\text{lead jet}} - p_T^{\text{sublead jet}})/(p_T^{\text{lead jet}} + p_T^{\text{sublead jet}}) , \quad (1)$$

where $p_T^{\text{lead jet}}$ and $p_T^{\text{sublead jet}}$ are the transverse momenta of the leading and sub-leading jet, respectively.

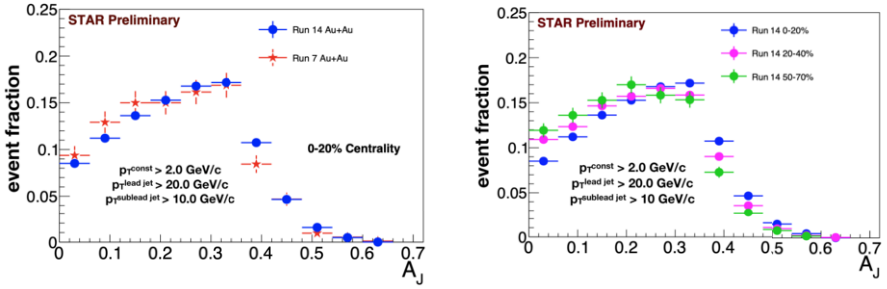

Fig. 1. (left) A_J distributions at detector level in 0 – 20% central Au+Au collisions from year 2007 [6] and 2014. (right) A_J distributions from year 2014 for three different centralities. Only statistical uncertainties are shown.

The di-jet momentum imbalance A_J is calculated for the leading and sub-leading jets with $p_T^{\text{lead jet}} > 20$ GeV/c, $p_T^{\text{sublead jet}} > 10$ GeV/c and $|\phi^{\text{lead jet}} - \phi^{\text{sublead jet}} - \pi| < 0.4$. Previous results [6] show that hard-core di-jets in central Au+Au collisions are significantly more imbalanced than the p+p di-jets. However, the momentum balance can be restored to the level of p+p baseline for resolution parameter R = 0.4 with soft particles included.

A large increase in the sample size obtained from year 2014 data allows us to study the centrality dependence of A_J. The left panel of Fig. 1 shows A_J distributions in 0 – 20% central Au+Au collisions from year 2007 (run 7) [6] and 2014 (run 14). In this analysis, jet energies are not corrected back to the original parton energies; all comparisons are done at detector level. The measured A_J distributions are relatively insensitive to the differences in the detector performance between year 2007 and 2014 and are comparable between the two years. The right panel of Fig. 1 shows A_J distributions from run 14 for three different centralities. An apparent evolution of the A_J distribution from central to peripheral collisions is observed where jets appear to be more balanced in peripheral Au+Au collisions.

3. Di-hadron Correlations

Measurements from both RHIC [6, 7, 8] and the LHC [9, 10] indicate that much of the lost energy of jets seems to re-emerge as low momentum particles. Redistribution of energy at low-to-modest p_T has been elusive to measure because of large flow background. We use a data-driven method for background evaluation and subtraction to measure the away-side jet-like correlation shape in heavy-ion collisions [11].

Because of the broad distribution of the underlying parton kinematics, the away-side jet direction is mostly uncorrelated in η relative to the trigger particle. It is therefore difficult to distinguish the jet signal from the underlying background. The away-side jet direction can be localized by requiring a second high-p_T particle back-to-back in azimuthal angle (ϕ) with respect to the trigger particle. However, by doing so, the back-to-back di-jets are biased towards being tangential to the collision zone, substantially weakening the

purpose of studying jet-medium interactions. In this analysis, we impose a less biasing requirement of a large recoil transverse momentum (P_x) azimuthally opposite to the high-p_T trigger particle, within a given range of pseudorapidity. P_x is given by

$$P_x|_{\eta_1}^{\eta_2} = \sum_{\eta_1<\eta<\eta_2, |\phi-\phi_{\rm trig}|>\pi/2} p_T \cos(\phi - \phi_{\rm trig}) \cdot \frac{1}{\epsilon}\,, \tag{2}$$

where all charged particles ($0.15 < p_T < 10$ GeV/c) within the η range that are on the away side ($|\phi - \phi_{\rm trig}| > \pi/2$) of the trigger particle are included. Since the near-side jet is not included in the P_x calculation, the η distribution of the trigger particle is unbiased by the P_x cut. The inverse of the single-particle relative acceptance×efficiency (ϵ) is used to correct for the relative single-particle detection efficiency. The requirement of a large recoil P_x in a particular η region selects events with enhanced population of jets close to the η region. In this analysis, the trigger particle p_T range is $3 < p_T^{\rm trig} < 10$ GeV/c. We choose the windows $-1 < \eta < -0.5$ ($P_x|_{-1}^{-0.5}$) or $0.5 < \eta < 1$ ($P_x|_{0.5}^{1}$) for P_x calculation.

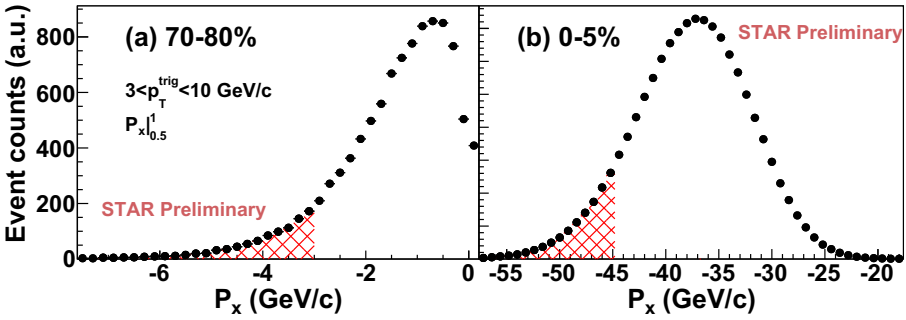

Fig. 2. Distributions of recoil momentum within $0.5 < \eta < 1$ ($P_x|_{0.5}^{1}$) from high-p_T trigger particles of $3 < p_T^{\rm trig} < 10$ GeV/c in 70-80% peripheral (a) and 0-5% central (b) Au+Au collisions at $\sqrt{s_{\rm NN}} = 200$ GeV. The shaded areas indicate a 10% selection of events with the highest $|P_x|$ to enhance the away-side jet-like population inside the acceptance. Statistical uncertainties only.

Figure 2 shows an example of $P_x|_{0.5}^{1}$ distributions for peripheral and central Au+Au collisions. Their difference comes mainly from event multiplicities. P_x has contributions from jets and anisotropic flow backgrounds. The flow background contribution is larger in central collisions which makes the P_x distribution more symmetric. For each centrality, we select the 10% of the events with the highest $|P_x|$ to enhance the away-side jet-like population. In the selected events, we analyze dihadron correlations of associated particles, with respect to trigger particles, in two η regions symmetric about mid-rapidity, one close to and the other far from the η window for P_x. For $P_x|_{-1}^{-0.5}$, the close-region is $-0.5 < \eta < 0$ and the far-region is $0 < \eta < 0.5$; for $P_x|_{0.5}^{1}$, they are swapped. The results from these two sets are combined. The away-side jet contributes more to the close region than to the far region due to the larger η gap of the latter. The anisotropic flow contributions, on the other hand, are on average equal in these two regions [12]. By focusing on the difference between close- and far-region correlations, we can therefore isolate jet-like correlations on the away-side.

The left panel of Fig. 3 shows the away-side correlation width (obtained as the Gaussian σ) as a function of centrality for four $p_T^{\rm assoc}$ bins. The width for the lowest $p_T^{\rm assoc}$ of 0.15-0.5 GeV/c is consistent with a constant over centrality; at such low $p_T^{\rm assoc}$, the correlations are fairly wide for all centralities and possible broadening with centrality may not be easily observable. For the three higher $p_T^{\rm assoc}$ bins, the width increases from peripheral to central collisions.

The right panel of Fig. 3 shows σ as a function of $p_T^{\rm assoc}$ in peripheral and central collisions. In peripheral collisions, the width decreases rapidly with $p_T^{\rm assoc}$. In central collisions the decrease is not as large. The right panel of Fig. 3 indicates stronger centrality dependence of broadening at higher p_T. In our measured $p_T^{\rm assoc}$ range, the away-side jet-like correlation broadening seems to display a different behavior than what was seen

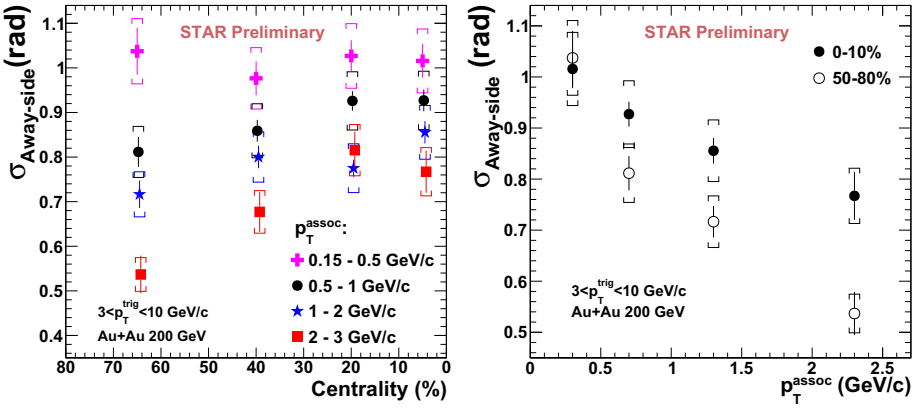

Fig. 3. (left) Away-side jet-like correlation width (Gaussian σ) as a function of centrality for $3 < p_T^{\text{trig}} < 10$ GeV/c and various p_T^{assoc} bins in Au+Au collisions at $\sqrt{s_{\text{NN}}} = 200$ GeV. The caps indicate the systematic errors. (right) Away-side jet-like correlation width as a function of p_T^{assoc} in peripheral and central collisions.

in jet-hadron correlations [7], which may be due to differences in kinematics and the selected trigger object. At higher p_T^{assoc} not covered by the current measurement, jet-hadron correlations, with much higher trigger (jet) p_T, indicate little broadening from proton-proton to central heavy-ion collisions. Relevant analysis of semi-inclusive hadron-jet correlations showed no evidence of significant intrajet broadening on the away-side within an angle of 0.5 relative to the jet axis [13].

4. Summary

In these proceedings, we presented the first measurement of centrality dependence of the di-jet momentum imbalance A_J at RHIC, with a clear evolution toward more balance in peripheral Au+Au collisions. A new measurement of away-side jet-like correlations is also reported with robust flow background subtraction. The correlation width broadens with increasing centrality except at low p_T. Stronger centrality dependence of away-side jet-like correlation broadening is observed at higher p_T.

Acknowledgements

This work was supported in part by the National Natural Science Foundation of China under Grant No. 11705194, the Anhui Provincial Natural Science Foundation under Grant No. 1808085QA23, and the Ministry of Science and Technology (MOST), China under Grant No. 2016YFE0104800.

References

[1] T. Renk, Phys. Rev. C 88 (2013) 054902.
[2] M. Anderson, et al., Nucl. Instrum. Meth. A499 (2003) 659–678.
[3] M. Beddo, et al., Nucl. Instrum. Meth. A 499 (2002) 725–739.
[4] M. Cacciari, et al., J. High Energy Phys 04 (2008) 005.
[5] M. Cacciari, et al., Eur. Phys. J. C72 (2012) 1896.
[6] L. Adamczyk, et al., Phys. Rev. Lett. 119 (6) (2017) 062301.
[7] L. Adamczyk, et al., Phys. Rev. Lett. 112 (12) (2013) 122301.
[8] A. Adare, et al., Phys. Rev. Lett. 111 (3) (2013) 032301.
[9] G. Aad, et al., Phys. Lett. B719 (2013) 220–241.
[10] S. Chatrchyan, et al., Phys. Lett. B712 (2012) 176–197.
[11] K. Jiang, Nucl. Part. Phys. Proc. 289-290 (2017) 354–357.
[12] V. Khachatryan, et al., Phys. Rev. C 92 (2015) 034911.
[13] L. Adamczyk, et al., Phys. Rev. C 96 (2017) 024905.